The 2017 World Congress on
Advances in Structural Engineering and Mechanics (ASEM17)
28 August - 1 September, 2017, Ilsan(Seoul), Korea

Interface behaviour of aluminium and Iron powder compacts at room temperature

Pragat P. Marathe[1)] Sharad V. Patil[2)] *Kanhu C. Nayak[3)] Prashant P. Date[4)] Alexander Pirumov[5)]

[1), 2), 3), 4)] *Department of Mechanical Engineering, IIT Bombay, Mumbai 400076, India*
[4)] *ppdate@iitb.ac.in*

[5)] *Department of Elektrotechnics and Mechanics, Moscow Technological University, Moscow 119526, Russia*

Abstract

Compacts from Al and iron powders were compressed under various loads such that their cylindrical surfaces touched that of the concentrically placed sleeve around the compact. Further compression led to development of frictional conditions between the compact and the sleeve. The variation of frictional force depended on the ductility of the material and the particle shape. The interfacial coefficient of friction showed no dependence on the material, and showed a power law relation with the axial force. The surface roughness (R_a) values varied along the height of the compacted aluminium powder sample from 4.5 to 6.64 microns, while the hardness ranged from 24 Hv to 11 Hv.

Keywords: friction test, friction, roughness, hardness, contact area

1. INTRODUCTION

Powder compacts are processed by extrusion for instance to impart the shape of the final product. The compact is initially compressed by free bulging until a slightly barrelled cylindrical surface comes in contact with the walls of the tool. As the material has to move forward, frictional forces would be expected to cause considerable shear deformation at the interface (and consequent work hardening of the surface layers) caused by large compressive forces leading to large normal force acting on the wall of the tool. Further increase in the compressive loading would cause the shear surface to move into the body of the billet thereby creating a thin shear surface on the cylindrical surface of the billet (sample). As the temperature increases, the shear strength of the

[4)] Corresponding author: Prof. P.P. Date, ppdate@iitb.ac.in
[*]Presenting author: Kanhu Charan Nayak, nayakkanhu83@gmail.com

billet would drop and the thin shear layer at the periphery of the billet would be formed at much lower loads. Besides, distribution of the strain rate across the thickness of the shear layer would depend upon the nature of the interface at relatively high temperatures.

Interface friction between solid metal and tool has been well studied in metal forming processes to enhance the quality of the surface of the product. The interface friction between product and tool, which decide the shear strain at that surface (Lyamina et al. 2007), affects surface quality of the product. A narrow layer at the boundary is developed where material properties are different from the properties in the bulk. Alexandrov (2005) has proposed a mathematical model based on the concept of strain-rate intensity factor to study the material properties at different regions on the frictional area. This approach was used for calculation of micro-hardness distribution developed by friction between tool and product (Lyamina et al. 2007), on the contact surface. Recently, Alexandrov et al. (2015) used the same mathematical approach based on strain rate intensity factor to analyse the direct extrusion of AZ31 alloy and determined the material properties near the friction surface. A hard narrow layer formed near the friction surface and they found the correlation between the thickness of this hard layer and strain intensity factor. However, the identification of this narrow friction affected layer is difficult for a powder compacted product that has undergone additional forming strain.

Solid and dry friction contacts are developed at the contact surface between tool and workpiece during the extrusion process. The mechanisms of friction present in tool-workpiece interaction are due to the formation of adhesive bonds (called molecular interactions) and the elastic and plastic deformation (called mechanical interaction). The friction at the tool-workpiece interface is the result of the sum total of molecular and mechanical interaction. In order to understand the frictional phenomena, recently some friction test have been developed like high-pressure friction test (Hora et al. 2012), torsion friction test and high speed friction test (Sanabria et al. 2014). The high-speed friction test was used for developing the sticking friction at the die and workpiece interface under different workpiece temperature (Sanabria et al. 2014) conditions. Properties like hardness and grain size at the surface were investigated for extruded AA6060 alloy. A thin hard layer with a small grain size (compared to the center of extruded workpiece) was also generated near the friction surface. Further, this friction test was used for extrusion of aluminium and magnesium alloy to understand the tool-workpiece interface friction behaviour (Sanabria et al. 2014). They analyzed the evolution of microstructure at different combinations of temperatures and friction speeds. In addition, the micro-hardness near the friction surface was studied.

However, in the entire test as mentioned in the literature, only solid wrought metallic workpieces have been used so far for the study of interface friction. It is necessary to understand the phenomena of friction in metallic powders in powder metallurgy technique. In powder metallurgy technique, many methods are like powder extrusion, powder forging and powder rolling are used to make products.

The present work focuses on the frictional behaviour of aluminium powder samples and those compacted from iron powder at room temperature. Compressive loads deployed are low to moderate and the frictional force is measured at room temperature.

In addition, hardness and roughness properties are determined and examined to know the effect of friction.

2. EXPERIMENTAL PROCEDURE

Two sets of powder compacted samples were fabricated. One set of the samples of green density 5.2g/cc was compacted from iron powder; another set of the green density of 2.1g/cc was compacted from aluminium powder.

The tool consisted of two opposing punches between which the sample was to be compressed, surrounded by a metallic sleeve to contain (enclose) the sample completely (Fig. 1). The top punch was longer than the bottom punch. Thus, on compressing the sample, an increase in diameter would be prevented by the cylindrical surface of the sleeve surrounding the sample, thereby generating a normal force (acting radially) between the cylindrical surface of the sleeve and that of the sample in contact.

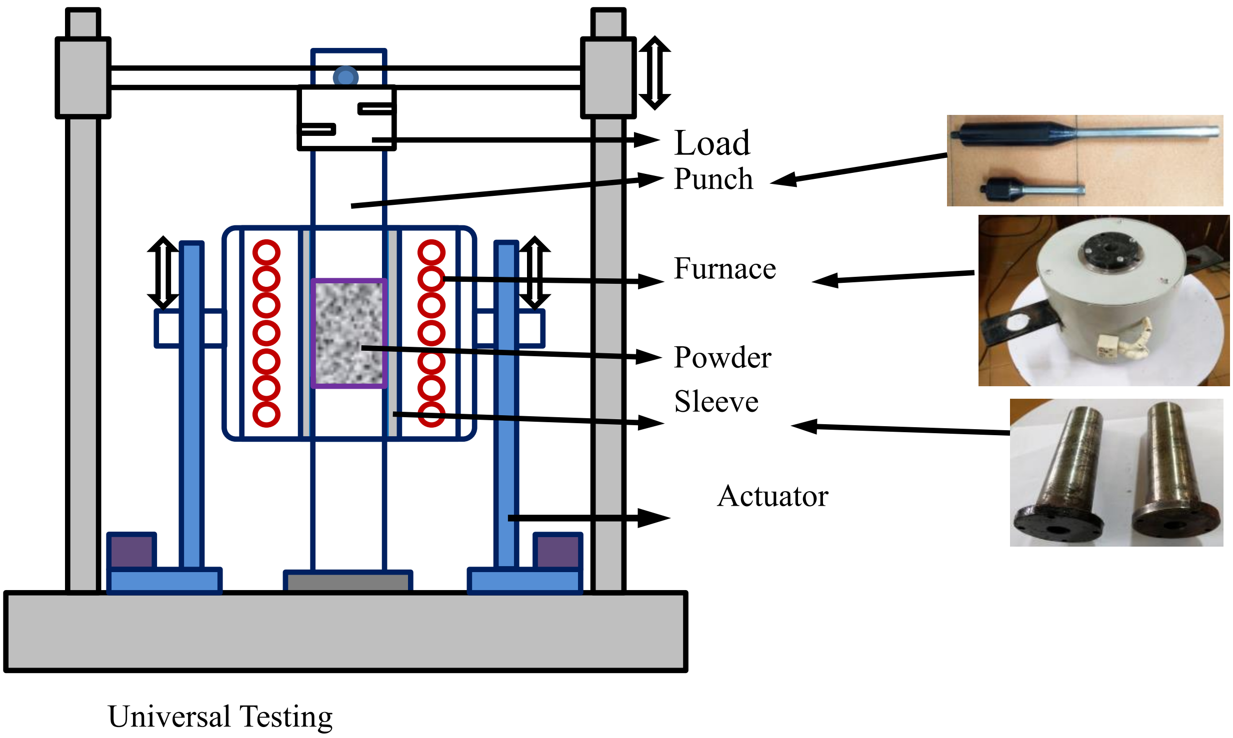

Fig. 1 A schematic of the experimental setup

Determining the area of contact is an important step. For this, blue colour was applied all over the cylindrical surface using an indelible ink. Wherever tool contact occurred, the ink was removed, and it remained behind in the other regions (Fig. 2). This enabled delineating regions of tool-workpiece contact from the non-contacting ones. The blue colour applied cylindrical compacted sample was compressed in between top and bottom punch surrounded by sleeve applying a certain amount of axial load. The maximum axial load varied from 25-29kN for aluminum compacted samples whereas for iron, it ranged from 18-22kN.

Thereafter, the sleeve was lifted up slowly at about 1mm/s. The force vs. time chart was recorded by the Tinius Olsen tensile testing machine. The specimens after axial compression under different loads are shown in Figs. 2(a)-(b). As the sleeve was moved relative to the compressed sample, a peak in the load was observed as shown in Figs. 3(a)-(b). This corresponds to the frictional force. The area of contact and the normal stress (calculated from the axial stress) was used to determine the normal force. This, together with the frictional force measured, was used to estimate the coefficient of friction.

Contrary to expectations, the area of contact was found to be non-uniform. This is seen from the sample in Figs. 2(a)-(b).

The load due to friction was higher when the sleeve was moved up as compared to when the sleeve was moved down (Fig. 3).

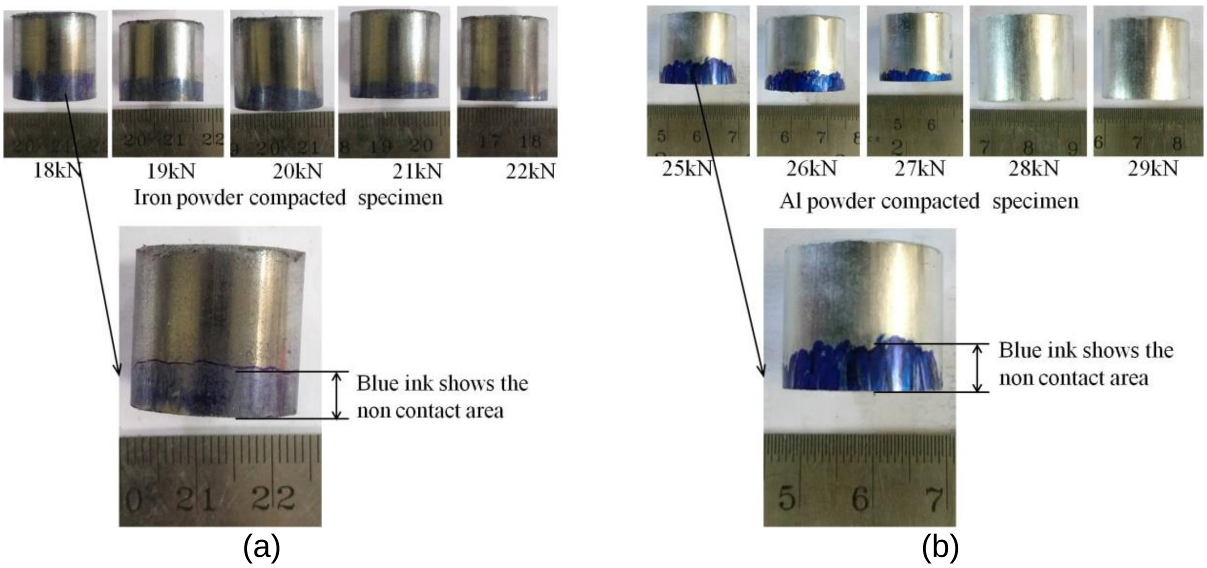

Fig. 2 The close up view of the tested sample for, (a) iron and (b) aluminium

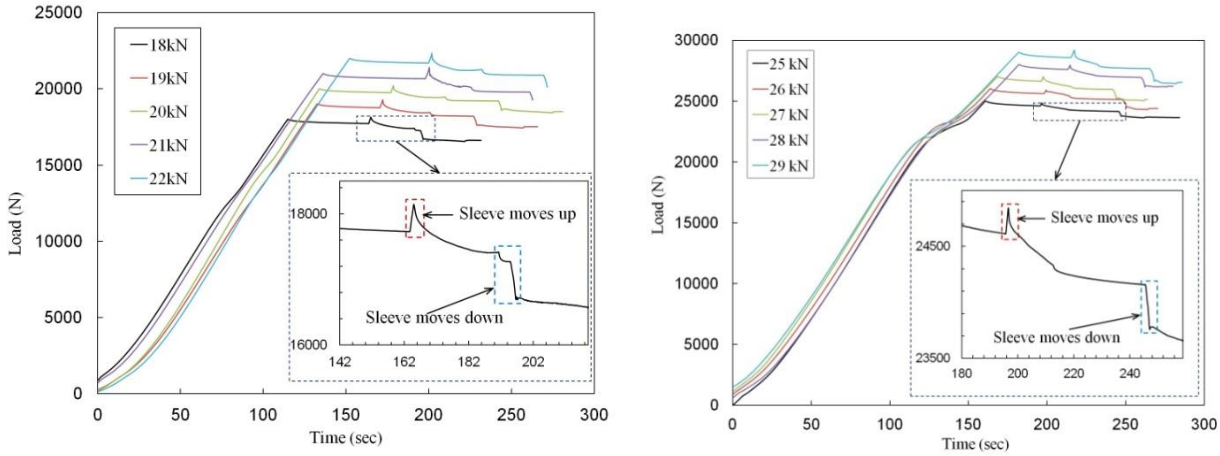

(a) (b)

Fig. 3 The short load peaks in the load time curves noticed from the load time recording and differences in the frictional load depending on which way the sleeve was moved for, (a) Iron and (b)aluminium

The procedure was repeated for two different materials (iron and aluminium). The experiment was repeated twice at each axial load for iron powder compacted samples and three times for aluminum powder compacted samples. The coefficient of friction on the cylindrical surface was determined in each case and the corresponding hardness at the contact interface was measured.

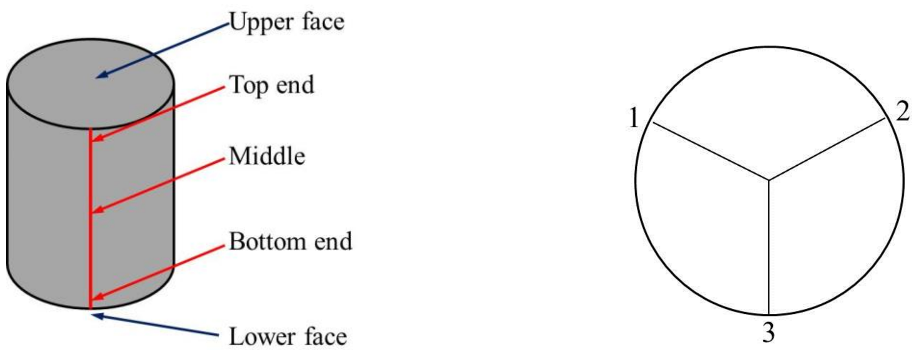

(a) (b)

Fig. 4. The scheme of measuring hardness and surface roughness for the flat and the cyindrical surfaces of the sample, (a) three positions along the axis and (b) three locations along the circumference for a given location along the axis

Surface roughness and surface hardness measurements were taken for the samples deformed. The surface roughness was measured on the cylindrical surface using a Zeta optical profilometer and Vicker's hardness was measured using a standard hardness tester (Vickers micro hardness, HMV2). The compacted sample was reversed when mounting for the friction test. Hence the face at the top end of the sample during compaction was as the bottom during the friction test. The top end during compaction showed the highest hardness and density of packing of the particles, and this was at on the lower platen for the friction test. A decrease in hardness is observed due to cylindrical surface getting abraded during the friction experiment due to the deformed (hardened) particles on the surface getting removed due to friction.

3. RESULTS AND DISCUSSIONS

Based on the experimental procedure of compacting metallic powders, compacts of 20mm diameter were made and compressed between a pair of flat platens using a plastic sheet as a solid lubricant between the platen and the workpiece. As the axial load increased, as expected, the compression increased the diameter of the sample. One would expect the surface roughness to increase with free bulging due to increasing circumferential strain, leading to a larger frictional coefficient at the time of contact with the sleeve. Hence, as the axial loading, and thus the contact pressure between the cylindrical surfaces of the sample and the sleeve is increased further, the normal force on the surface begins building up, the area of contact increases, the asperities get flattened and this shows as decreasing coefficient of friction. The specimen surface roughened by the initial free bulging gets smoothened in the area of contact. The percentage area of contact and the rate at which it approaches a value of 100% depends on the ductility (compressibility) of the powder. Aluminium powder for instance is more easily deformable compared to the iron powder. Hence the percentage of the specimen contact area in aluminium powder sample approaches closer to 100% than in case of the iron powder.

The axial force in excess of that needed for imminent contact is the driving force for the normal force of contact between the workpiece and the sleeve. The normal force is seen to increase linearly with this excess axial force (Fig. 5(a)). The rate of increase is greater for iron powder than for aluminium powder, and the maximum value of the normal force attained is greater for the iron compact compared to the aluminium compact. This is because, part of the energy of compression is used in deforming the powder particles, which serves to densify the aluminium powder compact. Thus the rate of increase in the normal force is relatively lower for aluminium powder compacts than that of iron powder. Inevitably, the shape of the powder particles would also influence this parameter.

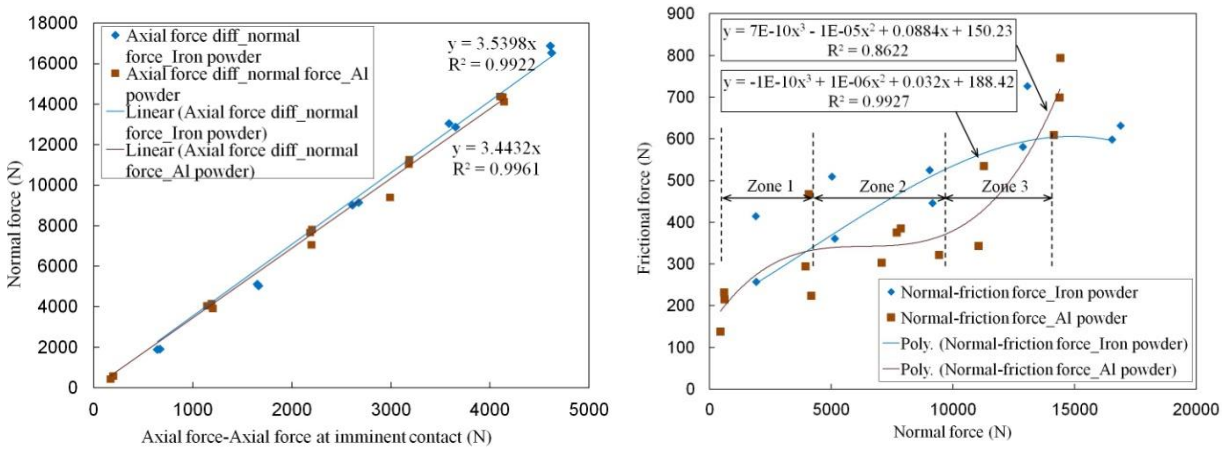

(a) Normal force varying with axial force (b) Frictional force varying with normal force

Fig. 5 Normal force varying with frictional force and axial force

The Frictional force-Normal force curve for Aluminium shows three zones of frictional behaviour. The frictional coefficient, which can be seen as the slope of the Frictional force-Normal Force curve (Fig. 5(b)), shows an initial high value followed by a sharp drop. This is followed by a gentle drop in the coefficient of friction consistent with a practically constant slope of the Frictional force-Normal force curve. An increase in the frictional coefficient depicted by a rise in the frictional force in zone 3 (at higher compressive loads) is not observed in the variation of the frictional coefficient seen in Fig. 5(b). Comparatively, in case of iron powder, the increase in the frictional force occurs at a decreasing rate with an increase in the normal force indicating a decrease in the coefficient of friction. The iron powder does not show a three stage behaviour as shown by the aluminium powder.

At a large axial force, the normal force on the surface of the sleeve increases. At relatively larger loads the elastic deflection of the sleeve would be the highest. While measuring the frictional force, as the sleeve is lifted, the point of contact on the sleeve will change thereby bringing an undeflected portion of the sleeve in contact with the sample maintained under a certain compressive load. Together with the fact that the elastic deflection in aluminium would be much greater than that in steel, this would lead to a greater 'frictional force' being measured in aluminium powder compact, despite flattening of the asperities on the cylindrical surface of the sample. Additionally, interlocking (proportional to the normal force) of the surface roughness profile of compacted soft, deformable aluminium particles with that of the steel sleeve would also lead to such an observation. With regard to iron powder, the loads involved are much greater, but the phenomenon of flattening of surface asperities of a free bulging iron compact on contact with the sleeve, and interlocking of the particles at the surface with the roughness profile of the sleeve would be far less than what was observed with aluminium powder which is softer and more deformable and compliant compared to iron. As a result, the frictional force increases with increasing axial (and hence normal) force in aluminium and much greater scatter is observed in the measured frictional force in view of the reasons just discussed.

The surface roughness (R_a) values varying along the height of the sample ranged from 4.5 to 6.64 microns, while the hardness ranged from 24 Hv to 11 Hv in the aluminium samples.

Examining Fig. 6, it is seen that the variation of coefficient of friction with the axial force in both Al and steel powders lies on the same curve. Hence the frictional behaviour of the two materials seems to be very similar after a relatively large surface contact between the sample and the sleeve, indicating the overwhelming influence of the powder properties and forming conditions compared to the material on the development of coefficient of friction.

Despite the above, the frictional force between the cylindrical surfaces of the samples (compacted from aluminium or iron powder) and the tool are very different. The frictional force at large axial force is seen to rise rapidly in case of aluminium compared to that of iron (Fig. 7).

The area of contact depends strongly on the nature of the powder (Fig. 8). Aluminium being a more easily deformable (softer) material shows a greater area of contact compared to that in an iron powder compact. Powder morphology too has a strong influence on the interlocking among particles. Together with a greater yield strength, this explains a relatively lower contact area compared to that of aluminium.

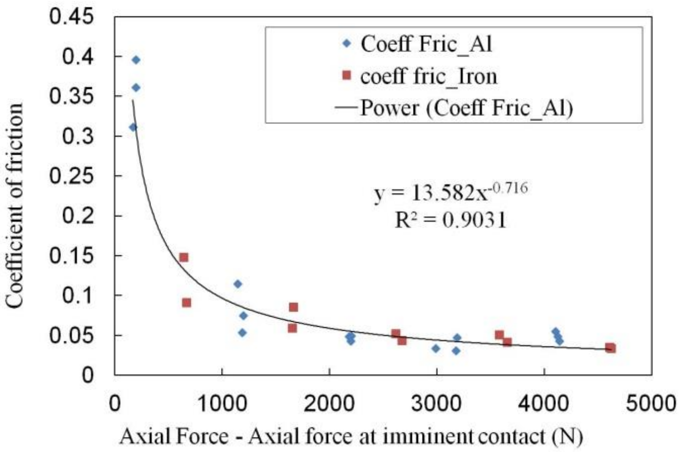

Fig. 6 Coefficient of friction with an increase in axial force for the two metal powders

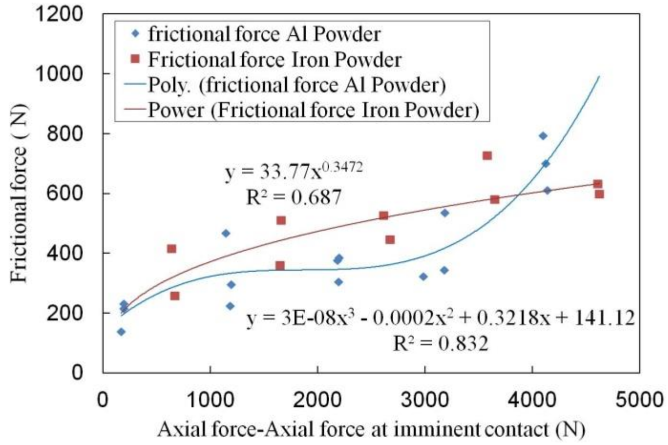

Fig. 7 Frictional force varying with axial force for powder compacts of iron and aluminium

Figs. 9(a)-(b) show the particle morphology for the aluminium powder (a) and the iron powder (b). Both the powders show a bimodal particle size, i.e., particles which can be divided into two classes - small sized particles and the large sized ones. The Al particles have a rounded shape and have well rounded edges, while those of iron are irregular in shape and show edges which are not rounded. This influences the interlocking among particles, and interparticle friction. Hence the compaction load increases without a significant increase in the percentage of area in contact with the sleeve. Besides, a relatively lower deformability of the iron particles leads to fragmentation of these particles under load.

Since the axial load after imminent contact would generate a normal contact force on the sleeve the magnitude of which would be subject to frictional resistance among particles, large scatter is observed in the variation frictional force with respect to the axial force for iron powder.

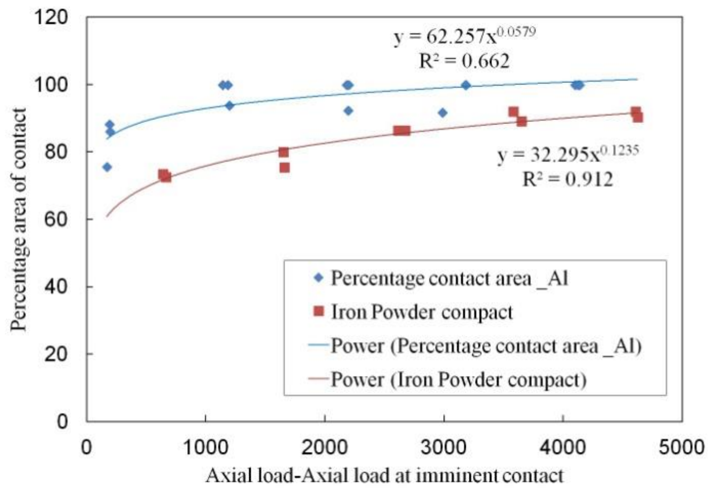

Fig. 8 Percentage area of contact with increasing axial load

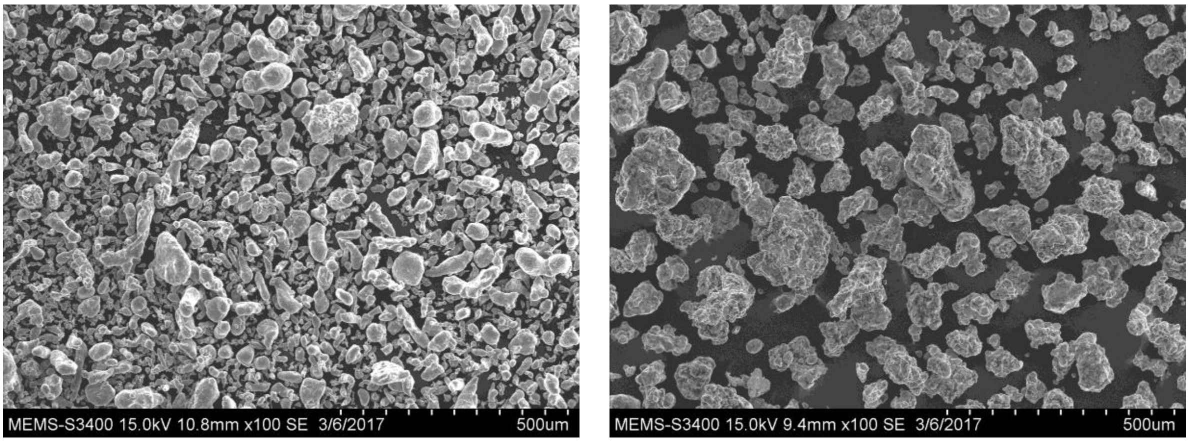

(a) (b)

Fig. 9 Powder particle morphology of (a) Aluminium powder and (b) Iron powder used in the study

4. CONCLUSIONS

From the foregoing observations and discussions, following conclusions emerge :

1. The various observations made on the basis of the axial friction test are well explained in light of results from the various investigations
2. The area of contact of the sample with the sleeve was always greater for aluminium powder compacts compared to those of iron powder.
3. The coefficient of friction decreases with an increase in the axial force, irrespective of the material.
4. The surface hardness after the friction test was found to be lower on account of removal of the hardened particles on the surface of the powder compacted samples.
5. The interface conditions at the room temperature strongly depend on the material of the powder, the particle morphology and the prior work hardening undergone by the particles.

Acknowledgements

The funding under the DST (INT/RUS/RFBR/P-214) for the experimental work conducted at IIT Bombay and RFBR (Project number 17-51-45085) Project is gratefully acknowledged.

References

Alexandrov, S. (2005), "An Approach to Predicting Evolution of Material Properties Near Surfaces With High Friction in Metal Forming" In *World Tribology Congress III*, Washington, September.

Alexandrov, S., Jeng, Y. R., and Hwang, Y. M. (2015), "Generation of a fine grain layer in the vicinity of frictional interfaces in direct extrusion of AZ31 alloy" *Journal of Manufacturing Science and Engineering*, Vol. **137**(5), 1-9.

Hora, P., Gorji, M., and Berisha, B. (2012), "Modeling of friction phenomena in extrusion processes by using a new torsion-friction test" *Key Engineering Materials*,Vol. **491**, 129-135.

Lyamina, E., Alexandrov, S., Grabco, D., and Shikimaka, O. (2007), "An approach to prediction of evolution of material properties in the vicinity of frictional interfaces in metal forming" *Key Engineering Materials*,Vol. **345**, 741-744.

Sanabria, V., Mueller, S., and Reimers, W. (2014), "A new high speed friction test for extrusion processes", *Key Engineering Materials*, Vol. **585**, 33-39.

Sanabria, V., Mueller, S., and Reimers, W. (2014), "Microstructure evolution of friction boundary layer during extrusion of AA 6060", *Procedia Engineering*, **81**, 586-591, 11th International Conference on Technology of Plasticity, Nagoya.

Sanabria, V., Mueller, S., Gall, S., and Reimers, W. (2014), "Investigation of friction boundary conditions during extrusion of aluminium and magnesium alloys" *Key Engineering Materials*, Vol. **611**, 997-1004.